BJP British Journal of Pharmacology

DOI:10.1111/j.1476-5381.2012.01980.x
www.brjpharmacol.org

RESEARCH PAPER

1-Dehydro-[10]-gingerdione from ginger inhibits IKKβ activity for NF-κB activation and suppresses NF-κB-regulated expression of inflammatory genes

Hwa Young Lee[1], Sun Hong Park[1], Misoon Lee[1], Hye-Jin Kim[2], Shi Yong Ryu[2], Nam Doo Kim[3], Bang Yeon Hwang[1], Jin Tae Hong[1], Sang-Bae Han[1] and Youngsoo Kim[1]

[1]*College of Pharmacy, Chungbuk National University, Cheongju, Korea,* [2]*Korea Research Institute of Chemical Technology, Daejeon, Korea, and* [3]*New Drug Development Center, Daegu-Gyeongbuk Medical Innovation Foundation, Daegu, Korea*

Correspondence
Dr Youngsoo Kim, College of Pharmacy, Chungbuk National University, Cheongju 361-763, Korea. E-mail: youngsoo@chungbuk.ac.kr

Keywords
ginger (*Zingiber officinale*); 1-dehydro-[10]-gingerdione; inhibitory κB kinase β; NF-κB; inflammatory gene; macrophages

Received
2 November 2011
Revised
24 February 2012
Accepted
27 March 2012

BACKGROUND AND PURPOSE

Pungent constituents of ginger (*Zingiber officinale*) have beneficial effects on inflammatory pain and arthritic swelling. However, the molecular basis for these pharmacological properties is only partially understood. Here, we investigated the molecular target of 1-dehydro-[10]-gingerdione (D10G), one of the pungent constituents of ginger, that mediates its suppression of NF-κB-regulated expression of inflammatory genes linked to toll-like receptor (TLR)-mediated innate immunity.

EXPERIMENTAL APPROACH

RAW 264.7 macrophages or primary macrophages-derived from bone marrows of C57BL/6 or C3H/HeJ mice were stimulated with the TLR4 agonist LPS in the presence of D10G. Catalytic activity of inhibitory κB (IκB) kinase β (IKKβ) was determined by a kinase assay and immunoblot analysis, and the expression of inflammatory genes by RT-PCR analysis and a promoter-dependent reporter assay.

KEY RESULTS

D10G directly inhibited the catalytic activity of cell-free IKKβ. Moreover, D10G irreversibly inhibited cytoplasmic IKKβ-catalysed IκBα phosphorylation in macrophages activated by TLR agonists or TNF-α, and also IKKβ vector-elicited NF-κB transcriptional activity in these cells. These effects of D10G were abolished by substitution of the Cys^{179} with Ala in the activation loop of IKKβ, indicating a direct interacting site of D10G. This mechanism was shown to mediate D10G-induced disruption of NF-κB activation in LPS-stimulated macrophages and the suppression of NF-κB-regulated gene expression of inducible NOS, COX-2 and IL-6.

CONCLUSION AND IMPLICATIONS

This study demonstrates that IKKβ is a molecular target of D10G involved in the suppression of NF-κB-regulated gene expression in LPS-activated macrophages; this suggests D10G has therapeutic potential in NF-κB-associated inflammation and autoimmune disorders.

Abbreviations

AP-1, activating protein 1; D10G, 1-dehydro-[10]-gingerdione; IκB, inhibitory κB; IKKβ, IκB kinase β; iNOS, inducible NOS; PTN, parthenolide; TNFSF11, receptor activator of NF-κB ligand; SEAP, secretory alkaline phosphatase; TLR, toll-like receptor

Introduction

Ginger (*Zingiber officinale*) is a member of the Zingiberaceae family of plants, and its rhizomes are commonly used as a spice or food supplement. Although often consumed for culinary purposes, some patients take ginger powder to ameliorate inflammatory pain and chronic swelling of osteoarthritis or rheumatoid arthritis (Bliddal *et al.*, 2000; Ali *et al.*, 2008). Ginger extract or its pungent constituents, including gingerol and shogaol, are also reported to have anti-inflammatory activities in experimental animal models (Levy *et al.*, 2006; Fouda and Berika, 2009). The mechanism of the anti-inflammatory action of ginger was first confirmed to be due to dual inhibition of COX and 5-lipoxygenase, enzymes essential for arachidonate metabolism (Kiuchi *et al.*, 1992), and then extended to down-regulation of the induction of inflammatory genes (Ali *et al.*, 2008; Tripathi *et al.*, 2008). The latter effect means that ginger can modulate pathophysiological pathways activated in chronic inflammation. However, the molecular targets of ginger involved in the suppression of inflammatory genes are only partially understood.

Toll-like receptors (TLR) are involved in the innate immune response and play pivotal roles in inflammation and the initiation of the subsequent immune response (Ospelt and Gay, 2010). TLR ligands stimulate the cellular activity of NF-κB through adaptor molecules, such as the myeloid differentiation primary-response gene 88 (MyD88), at an early time point and the Toll/ IL-1 receptor domain-containing adaptor-inducing IFN-β (TRIF) in delayed kinetics (Shen *et al.*, 2008). Under normal conditions, NF-κB is sequestered in the cytoplasm as an inactive complex bound to inhibitory κB (IκB) proteins (Baeuerle and Baltimore, 1988). Upon stimulation with a TLR2/6, TLR4 or TLR5 agonist, macrophages or other target cells phosphorylate cytoplasmic IκBs: this is induced by the catalytic activity of IκB kinase β (IKKβ) (DiDonato *et al.*, 1996). These phospho (p)-IκBs are then degraded by proteasome, after which NF-κB is translocated into the nucleus (Karin and Ben-Neriah, 2000). Nuclear NF-κB binds to the κB motifs on promoter regions of inflammatory genes, including inducible NOS (iNOS), COX-2 and IL-6, for transcriptional activation (Tian and Brasier, 2003). Therefore, NF-κB is an attractive therapeutic target for inflammatory and autoimmune disorders.

[6]-Gingerol from ginger suppresses iNOS expression by inhibiting IκBα phosphorylation in macrophages activated by the TLR4 agonist LPS (Lee *et al.*, 2009). It has also been shown to inhibit COX-2 expression, by blocking p38 MAPK-mediated phosphorylation of IκBα or the NF-κB p65 subunit, in phorbol ester-treated mouse skin (Kim *et al.*, 2005). [6]-Shogaol from ginger suppresses NF-κB-regulated gene expression of iNOS and COX-2 in LPS-activated macrophages by targeting the activation of PI3K, p44/42 MAPK and IKKβ (Pan *et al.*, 2008). 1-Dehydro-[10]-gingerdione (D10G, Figure 1A) from ginger is more effective than [6]-shogaol and other pungent constituents at inhibiting the production of NO in LPS-activated macrophages (Koh *et al.*, 2009). In a preliminary study, D10G also inhibited LPS-induced NF-κB transcriptional activity in macrophages, and it displayed the highest inhibitory effect among the pungent isolates from ginger (Figure S1). The current study was designed to elucidate the molecular mechanism by which D10G is able to suppress the NF-κB-regulated expression of inflammatory genes linked to TLR-mediated innate immunity. Treatment with D10G directly inhibited IKKβ activity by targeting the activation loop of IKKβ, thus disrupting IKKβ-catalysed IκBα phosphorylation in macrophages stimulated with TLR2/6, TLR4 or TLR5 agonists. This effect of D10G mediated the suppression of NF-κB-regulated expression of inflammatory genes such as iNOS, COX-2 and IL-6 in these stimulated cells.

Methods

Chemicals, antibodies and plasmids

D10G (>95% purity) was isolated from ginger (*Z. officinale*) as described previously (Koh *et al.*, 2009). In brief, the dried rhizomes of *Z. officinale* were extracted with 70% methanol and then partitioned with H_2O : dichloromethane (1:1). The dichloromethane fraction was repetitively subjected to chromatographic purification using a silica gel column. Purity of D10G was determined by HPLC analysis (Figure S2). Primary and secondary antibodies used in this study were purchased from Cell Signaling Tech (Danvers, MA, USA) or Santa Cruz Biotech (Santa Cruz, CA, USA). A NF-κB-dependent reporter construct of pNF-κB-secretory alkaline phosphatase-neomycin phosphotranferase (pNF-κB-SEAP-NPT) and promoter-dependent reporter plasmids of piNOS (−1592/+183)-Luc or pCOX-2 (−963/+1)-Luc were as previously described (Lowenstein *et al.*, 1993; Moon *et al.*, 2001; Yeo *et al.*, 2003). All other chemicals including TLR agonists were purchased from Sigma-Aldrich (St. Louis, MO, USA).

Cell culture

RAW 264.7 macrophages were purchased from ATCC (Manassas, VA). Primary macrophages were prepared from bone marrows of C57BL/6 or C3H/HeJ mice as described previously (Chung *et al.*, 2010). All studies involving animals are reported in accordance with the ARRIVE guidelines (Kilkenny *et al.*, 2010;McGrath *et al.*, 2010). Animal experiments were carried out following the protocols approved by Animal Experimentation Ethics Committee in CBNU institute. Macrophages were grown in DMEM containing 10% FBS, benzylpenicillin potassium (143 $U \cdot mL^{-1}$) and streptomycin sulfate (100 $\mu g \cdot mL^{-1}$) at 37°C and 5% CO_2. RAW 267.4 cells harbuoring the pNF-κB-SEAP-NPT construct were cultured in the same media with an additional supplement of geneticin (500 $\mu g \cdot mL^{-1}$).

IKKβ kinase assay

Ser/Thr kinase activity of IKKβ was determined as described previously (Kim *et al.*, 2008). In brief, IKKβ proteins were reacted with substrate GST-IκB (2 μg) and co-factor [γ-^{32}P]-ATP (5 μCi) in a kinase buffer (20 mM HEPES, pH 7.7, 2 mM $MgCl_2$, 50 μM ATP, 10 mM β-glycerophosphate, 10 mM NaF, 300 $\mu g \cdot mL^{-1}$ Na_3VO_4, 2 μM PMSF, 10 $\mu g \cdot mL^{-1}$ aprotinin, 1 $\mu g \cdot mL^{-1}$ leupeptin, 1 $\mu g \cdot mL^{-1}$ pepstatin) at 30°C for 1 h. These reaction mixtures were resolved on SDS-acrylamide gels by electrophoresis. Radioactive bands from the dried gels were then visualized by exposure to X-ray film. Wild-type IKKβ proteins were purchased from Millipore (Billerica, MA,

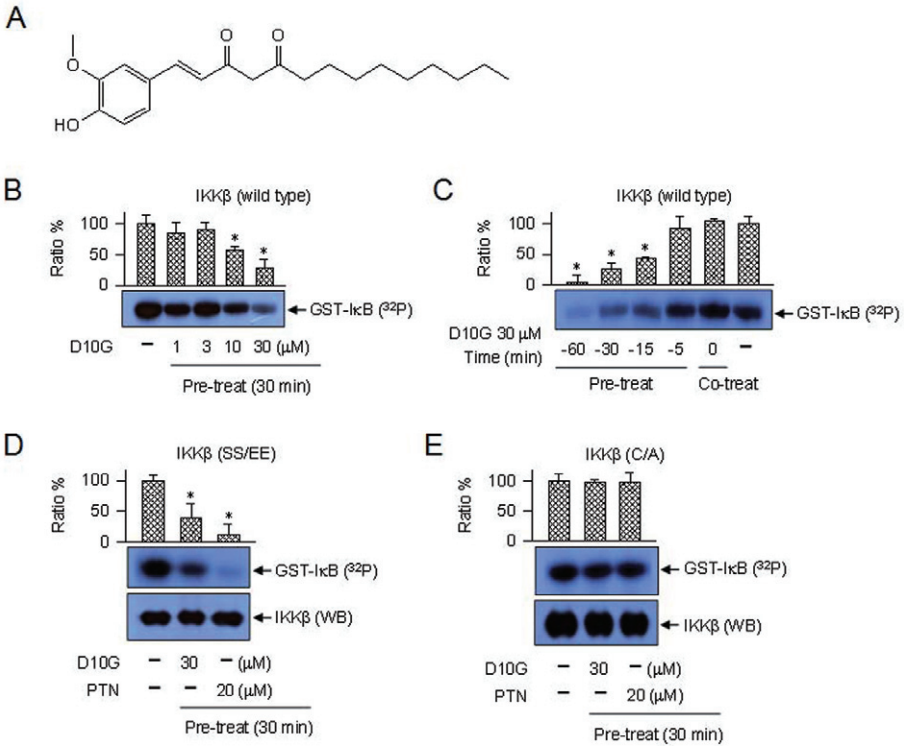

Figure 1

Effect of D10G on IKKβ activity. (A) Chemical structure of D10G. (B) Wild-type IKKβ proteins were pretreated with D10G for 30 min and then reacted with substrate GST-IκB and cofactor ATP. Catalytic activity of the enzyme was measured by GST-IκB phosphorylation (^{32}P). (C) Wild-type IKKβ proteins were pretreated with D10G at 30 μM for the indicated times and then subjected to the kinase reaction for GST-IκB phosphorylation (^{32}P). RAW 264.7 cells were transfected with FLAG-tagged expression vector encoding point-mutated IKKβ protein, IKKβ (SS/EE) (D) or IKKβ (C/A) (E). Cell extracts were immunoprecipitated with anti-FLAG M2 affinity gel freezer-safe beads. These immunoprecipitates were pretreated with D10G or parthenolide (PTN) for 30 min and then subjected to the kinase reaction for GST-IκB phosphorylation (^{32}P) and Western blot analysis (WB) normalizing IKKβ levels in the immunoprecipitates. Data are represented as the relative ratio %, mean ± SD of three independent experiments, in which the density of the IKKβ alone-treated group is expressed as 100%. *$P < 0.05$ versus IKKβ alone-containing group.

USA). For preparing point-substituted IKKβ proteins, RAW 264.7 cells were transfected with FLAG-tagged expression vector encoding IKKβ (SS/EE) with Glu residues instead of Ser^{177} and Ser^{181} or IKKβ (C/A) with Ala residue instead of Cys^{179} (Kim *et al.*, 2008). Point-substituted IKKβ proteins were precipitated from cell extracts using anti-FLAG affinity gel freezer-safe beads, washed with 20 mM HEPES (pH 7.7) and then subjected to the kinase assay.

Immunoblot analysis

Cell extracts were resolved on SDS-acrylamide gels by electrophoresis and then transferred to a PVDF membrane. Either 5% non-fat milk in PBS with Tween 20 or 5% BSA in Tris-buffered saline with Tween 20 was used as the blocking buffer. The blots were reacted at 4°C overnight with primary antisera (dilution): anti-IKKβ (1:200), anti-p-IκBα (1:300), anti-IκBα (1:1000), anti-iNOS (1:1500), anti-COX-2 (1:1500) or anti-GAPDH (1:2000). The blots were then incubated with appropriate HRP-labelled secondary antisera (1:2500) at room temperature for 2–5 h. These immune complexes were visualized by exposure to X-ray film after reacting with an enhanced chemiluminescence reagent (GE Healthcare, Chalfont St Giles, UK).

SEAP reporter assay

RAW 264.7 cells containing the pNF-κB-SEAP-NPT construct were stimulated with LPS (1 μg·mL^{-1}) or the receptor activator of NF-κB ligand (TNFSF11, RANKL) 40 ng·mL^{-1} for 20 h in the presence of D10G. SEAP expression, a reporter of NF-κB transcriptional activity, was measured as described previously (Moon *et al.*, 2001). In brief, aliquots of the culture media were heated at 65°C for 5 min and then reacted with 4-methylumbelliferyl phosphate (500 μM) in the dark. SEAP activity was measured as the relative fluorescence units (RFUs) with emission at wavelength 449 nm and excitation at wavelength 360 nm. Separately, RAW 264.7 cells containing the pNF-κB-SEAP-NPT construct were transfected with the expression vector encoding IKKβ (SS/EE) or IKKβ (C/A) in combination with pSV-β-galactosidase control vector, using lipofectamine (Invitrogen, Carlsbad, CA, USA) according to the manufacturer's protocol. These cells were treated with D10G for 20 h. Aliquots of culture media were subjected to SEAP reporter assay and cell extracts to β-galactosidase assay, in which SEAP activity was normalized to β-galactosidase activity for determining transfection efficiency.

Molecular modelling

The D10G–IKKβ covalent bound complex was built using the crystal structure of human IKKβ (Protein Data Bank accession code 3QA8). D10G was introduced into the Cys^{179} of IKKβ by visual manipulation. Energy minimization of the D10G–IKKβ complex was carried out using the steepest descent method, the minimization step was set as 1000, and final convergence was set as 0.01 $kcal \cdot mol^{-1} \cdot Å^{-1}$. The calculations were performed with OPLS-2005 force field in MacroModel. Molecular graphics for the D10G–IKKβ covalent bound complex were generated using the PyMol package (DeLano Scientific, San Carlos, CA, USA).

Confocal microscopy

RAW 264.7 cells were fixed in 4% *p*-formaldehyde, permeabilized in 0.5% Triton X-100 and then blocked in 1% BSA. For immunostaining, these cells were incubated with anti-NF-κB p65 antibody for 2 h and then reacted with Alexa Fluor 568-labelled secondary antibody (Invitrogen). For nuclei staining, the cells were also incubated with DAPI solution, and then analysed under a confocal fluorescence microscope.

Cell proliferation assay

RAW 264.7 cells were incubated with D10G for 24 h in the presence of LPS (1 $\mu g \cdot mL^{-1}$) and then reacted with water-soluble WST-1 (500 μM) of 2-(4-iodophenyl)-3-(4-nitrophenyl)-5-(2,4-disulfonyl)-2*H*-tetrazolium (Dojindo Lab, Kumamoto, Japan) for 3–4 h. Absorbance values were measured at wavelength 450 nm.

RT-PCR analysis

Total RNAs were subjected to RT-PCR using an RNA PCR kit (Solgent, Daejeon, Korea). In brief, total RNAs were reverse transcribed at 42°C for 1 h and then subjected to 25–30 cycles of PCR consisting of 30 s denaturation at 94°C, 30 s annealing at 50–60°C and 90 s extension at 72°C. Nucleotide sequences of RT-PCR primers and the sizes of PCR products are as follows: iNOS, sense 5′-GTCAACTGCAAGAGAACGG AGAC-3′, anti-sense 5′-GAGCTCCTCCAGAGGGTAGGCTTG-3′, 457 base pair (bp); COX-2, sense 5′-ACTCACTCAGTT TGTTGAGTCATTC-3′, anti-sense 5′-TTTGATTAGTACTGTA GGGTTAATG-3′, 583 bp; IL-6, sense 5′-ATGAAGTTCCTC TCTGCAAGAGACT-3′, anti-sense 5′-CCTTCTGTGACTCCA GCTTATCTGT-3′, 549 bp; and β-actin, sense 5′-CACCACA CCTTCTACAATGAGCTGC-3′, anti-sense 5′-GCTCAGGAGG AGCAATGATCTTGAT-3′, 745 bp. RT-PCR products were resolved on agarose gels by electrophoresis and then visualized by staining with ethidium bromide.

Luciferase reporter assay

RAW 264.7 cells were transiently transfected with each luciferase reporter construct of piNOS (–1592/+183)-Luc, pCOX-2 (–963/+1)-Luc or pAP-1-Luc, in combination with *Renilla* control vector, using lipofectamine. These cells were then stimulated with LPS (1 $\mu g \cdot mL^{-1}$) for 20 h in the presence of D10G. Cell extracts were subjected to dual-luciferase assay (Promega, Madison, WI, USA), in which firefly luciferase activity was normalized to *Renilla* activity.

ELISA

RAW 264.7 cells were stimulated with LPS (1 $\mu g \cdot mL^{-1}$) for 24 h in the presence of D10G. The concentrations of IL-6 or PGE_2 in the culture media were determined using an ELISA kit (R&D Systems, Minneapolis, MN, USA).

NO quantification

RAW 264.7 cells were stimulated with LPS (1 $\mu g \cdot mL^{-1}$) or TNFSF11 (40 $ng \cdot mL^{-1}$) for 24 h in the presence of D10G, and then the concentrations of nitrite, a stable metabolite of NO, were determined. In brief, aliquots of the culture media were reacted with 0.1% sulfanilamide and 0.1% *N*-(1-naphthyl) ethylenediamine in 5% phosphoric acid. Absorbance values were measured at wavelength 540 nm with $NaNO_2$ as a standard.

Statistical analysis

Data are expressed as mean ± SD of at least three independent experiments and were subjected to one-way ANOVA followed by Dunnett's test. $P < 0.05$ was considered as statistically significant.

Results

D10G inhibits catalytic activity of IKKβ

The IKKβ-catalysed phosphorylation of cytoplasmic IκB proteins plays a pivotal role in the activation of NF-κB in inflammatory responses or other cellular activities (Schmid and Birbach, 2008). Firstly, we examined whether D10G can directly affect the Ser/Thr kinase activity of cell-free IKKβ. Wild-type IKKβ proteins were pretreated with D10G for 30 min and then reacted with substrate GST-IκB and co-factor ATP to determine the catalytic activity for GST-IκB phosphorylation. Treatment with D10G inhibited the IKKβ-catalysed GST-IκB phosphorylation in a dose-dependent manner (Figure 1B). To better understand the time it takes for D10G to inactivate IKKβ, we carried out a time course study. Pretreatment of IKKβ with D10G (30 μM) for 1 h completely inhibited its *in vitro* kinase activity in the presence of a substrate, whereas pre-incubation for 15–30 min exhibited about 60–75% inhibition and co-treatment in the presence of substrate yielded no inhibition (Figure 1C). Therefore, D10G was an efficient inhibitor of IKKβ activity only when it was pre-incubated with the enzyme source before the kinase reaction *in vitro*.

Some thiol-reactive chemicals such as parthenolide (PTN; Figure S3) directly interact with the Cys^{179} in the activation loop of IKKβ through Michael addition (Hehner *et al.*, 1999; Gupta *et al.*, 2010). D10G also contains a good electrophile in its α,β-unsaturated carbonyl structure (Figure 1A). Hence, we determined whether D10G inhibits the catalytic activity of IKKβ by a direct interaction with the activation loop of IKKβ. To address this issue, we transfected RAW 264.7 cells with a FLAG-tagged expression vector encoding IKKβ (SS/EE) or IKKβ (C/A). The IKKβ (SS/EE) is a point-substituted IKKβ with Glu residues instead of two Ser^{177} and Ser^{181} of IKKβ that function as phosphate acceptors to become more active on stimulation of its kinase activity (Mercurio *et al.*, 1999). The IKKβ (C/A) is

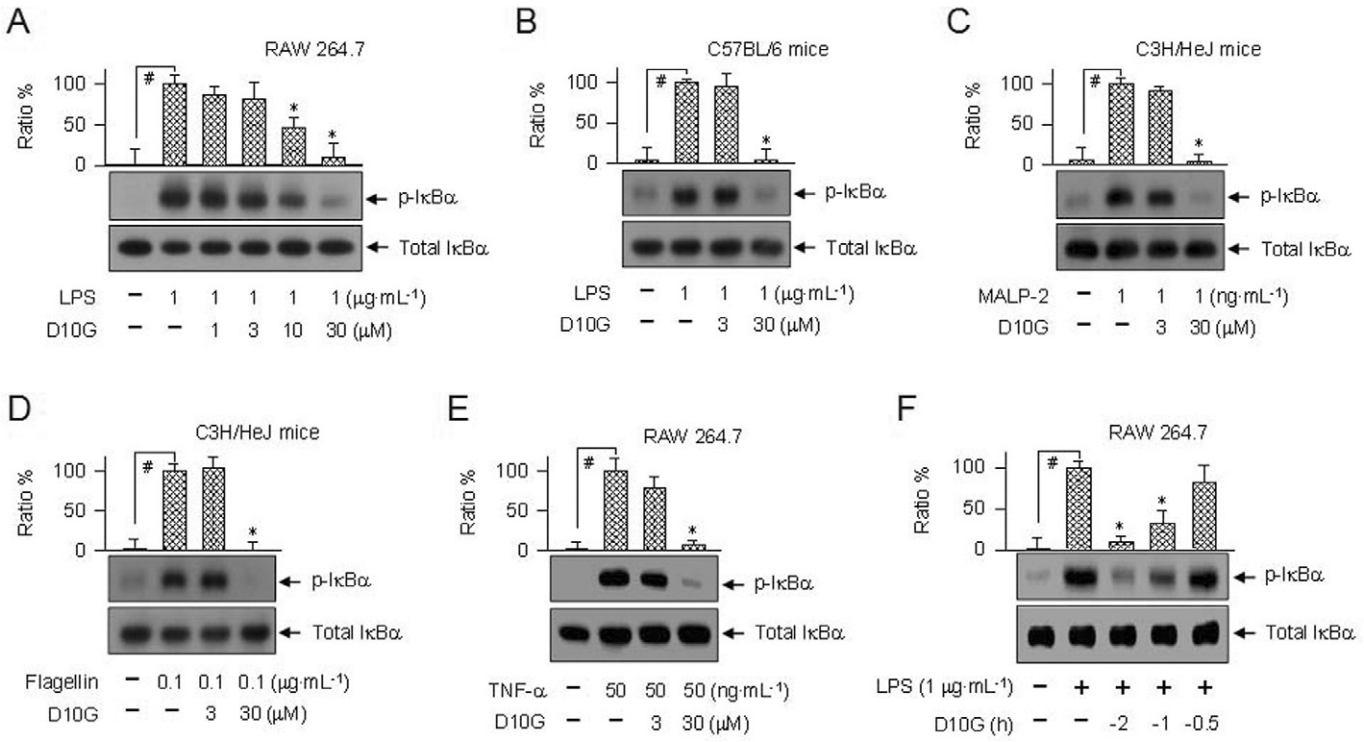

Figure 2

Effect of D10G on TLR agonist- or TNF-α-induced IκBα phosphorylation. RAW 264.7 cells (A) or primary macrophages-derived from C57BL/6 mice (B) were pretreated with D10G for 2 h and stimulated with the TLR4 agonist LPS for 10 min in the presence of D10G. Primary macrophages derived from C3H/HeJ mice were pretreated with D10G for 2 h and stimulated with the TLR2/6 agonist MALP-2 (C) or TLR5 agonist flagellin (D) for 15–20 min in the presence of D10G. (E) RAW 264.7 cells were pretreated with D10G for 2 h and stimulated with TNF-α for 10 min in the presence of D10G. (F) RAW 264.7 cells were pretreated with D10G at 30 μM for 30 min to 2 h, followed by washing the cells and recovery in the complete media for 1 h. These cells were then stimulated with LPS alone for 10 min. Cell extracts were subjected to Western blot analysis with anti-p-IκBα or anti-IκBα antibody. The p-IκBα levels are represented as a relative ratio % after normalizing to total IκBα. Data are expressed as mean ± SD of three independent experiments. $^{\#}P < 0.05$ versus media alone-added group. $^{*}P < 0.05$ versus TLR agonist or TNF-α alone-stimulated group.

another point-substituted IKKβ with Ala residue instead of Cys^{179}. The Cys^{179} residue of IKKβ is often altered by thiol-reactive inhibitors (Byun *et al.*, 2006). These point-substituted IKKβ proteins were immunoprecipitated with anti-FLAG antibody from the cell extracts. They still exhibited catalytic activity for GST-IκB phosphorylation *in vitro*, and IKKβ (SS/EE) showed much higher kinase activity than IKKβ (C/A) as expected (Figure 1D, E). Treatment with D10G inhibited the catalytic activity of IKKβ (SS/EE) immunoprecipitates, as did the positive control PTN (Figure 1D). In contrast, treatment with D10G or PTN had no apparent effect on the kinase activity of IKKβ (C/A) immunoprecipitates (Figure 1E). These findings suggest that D10G might directly interact with Cys^{179} in the activation loop of IKKβ, thus inhibiting the catalytic activity of cell-free IKKβ.

D10G inhibits TLR- or TNF-α-mediated IκBα phosphorylation in macrophages

To understand whether D10G can also inhibit IKKβ activity in intact cells, we stimulated macrophages with various TLR agonists or TNF-α in the presence of D10G and then performed Western blot analysis with anti-p-IκBα or anti-IκBα antibody. Upon stimulating TLR4 with LPS alone for 10 min, macrophages markedly phosphorylated the Ser^{32} and Ser^{36} of cytoplasmic IκBα under conditions prior to IκBα degradation (Figure 2A, B). Treatment with D10G dose-dependently inhibited LPS-induced IκBα phosphorylation in RAW 264.7 cells (Figure 2A) and also in primary macrophages derived from C57BL/6 mice (Figure 2B). Moreover, D10G inhibited not only TLR2/6 agonist MALP-2- or TLR5 agonist flagellin-induced IκBα phosphorylation in primary macrophages derived from C3H/HeJ mice (Figure 2C, D) but also TNF-α-induced IκBα phosphorylation in RAW 264.7 cells (Figure 2E). However, LPS alone or treatment with D10G did not induce or affect IκBα phosphorylation in primary macrophages derived from C3H/HeJ mice (data not shown), which have a missense mutation disrupting TLR4 function (Poltorak *et al.*, 1998). We next asked whether the effect of D10G on cellular IKKβ-catalysed IκBα phosphorylation is irreversible or not. RAW 264.7 cells were pre-incubated with D10G for various time periods ranging from 30 min to 2 h, then washed, allowed to recover in complete media for 1 h and stimulated with LPS for 10 min. Treatment with D10G still inhibited LPS-induced IKKβ activity phosphorylating

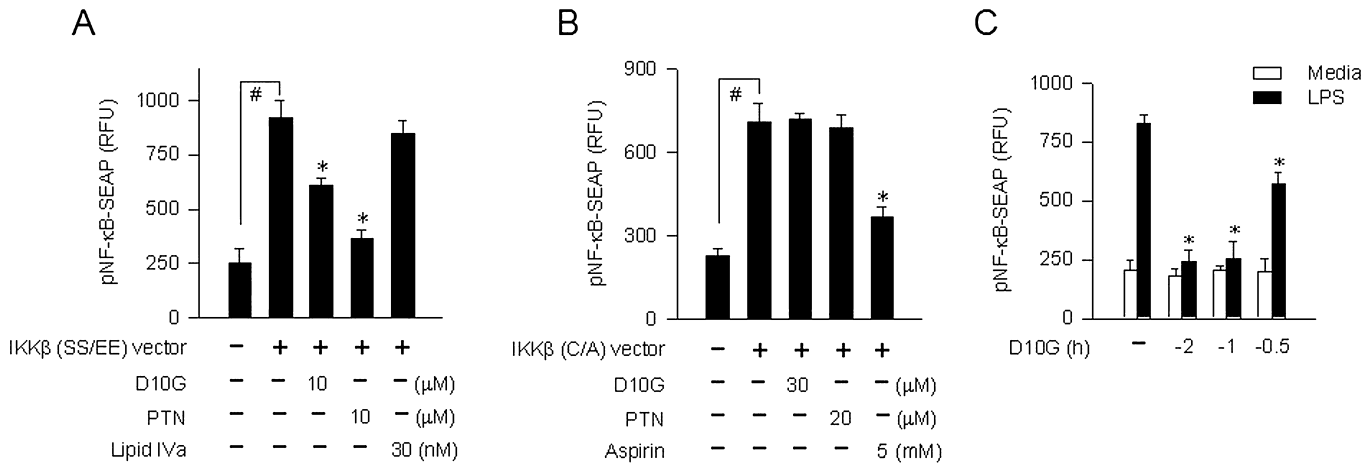

Figure 3

Effect of D10G on IKKβ vector-elicited NF-κB transcriptional activity. RAW 264.7 cells containing pNF-κB-SEAP-NPT reporter construct were transfected with an expression vector encoding IKKβ (SS/EE) (A) or IKKβ (C/A) (B) in combination with pSV-β-galactosidase control vector. These transfected cells were treated with D10G, parthenolide (PTN), lipid IVa or aspirin for 20 h. (C) RAW 264.7 cells containing pNF-κB-SEAP-NPT reporter construct were pretreated with D10G at 30 μM for 30 min to 2 h, followed by washing the cells and then recovering in the complete media for 1 h. These cells were then incubated for 20 h in the absence or presence of LPS (1 μg·mL^{-1}). SEAP expression as a reporter of NF-κB transcriptional activity was measured as relative fluorescence units (RFU). Data are expressed as mean ± SD of three to five independent experiments. $^{\#}P < 0.05$ versus media alone-added group. $^{*}P < 0.05$ versus IKKβ expression vector alone-transfected group (A, B) or LPS alone-stimulated group (C).

cytoplasmic IκBα even after it was removed from the cells before stimulation with LPS (Figure 2F). Therefore, D10G inhibited cytoplasmic IKKβ-catalysed IκBα phosphorylation, a converging step in the TLR2/6, TLR4, TLR5 or TNF-α-induced NF-κB activating pathways in macrophages, and its mechanism of action was irreversible.

D10G inhibits cellular NF-κB activation elicited by IKKβ expression vector

To confirm that D10G can really interact with the activation loop of IKKβ inside the cells, we transfected RAW 264.7 cells containing the pNF-κB-SEAP-NPT construct, a SEAP reporter fused to four copies of the NF-κB-responsive κB motifs (Moon *et al.*, 2001), with the expression vector encoding IKKβ (SS/EE) or IKKβ (C/A), and then treated these cells with D10G. Ectopic expression of IKKβ (SS/EE) or IKKβ (C/A), which bypasses TLRs, increased SEAP expression as a reporter of NF-κB transcriptional activity over the basal levels (Figure 3A, B). Treatment with D10G inhibited the IKKβ (SS/EE) vector-elicited SEAP expression in these macrophages, in which IKKβ inhibitor PTN was also effective but the TLR4 antagonist lipid IVa (Ohto *et al.*, 2007) was inert as expected (Figure 3A). In contrast, treatment with D10G or PTN did not affect the IKKβ (C/A) vector-elicited SEAP expression but aspirin, another IKKβ inhibitor targeting ATP binding site (Yin *et al.*, 1998), was effective as expected (Figure 3B). These cellular results with IKKβ vectors were consistent with the *in vitro* readouts of kinase activities with point-substituted IKKβ proteins. Furthermore, treatment with D10G still showed significant inhibitory effects on the LPS-induced NF-κB transcriptional activity even after it was washed out from the cells before stimulation with LPS (Figure 3C), also indicating its irreversible mechanism of action. From these results we concluded that D10G inhibits NF-κB transcriptional activity induced by an IKKβ vector or LPS in an irreversible mechanism by directly interacting with Cys^{179} in the activation loop of IKKβ.

Molecular docking of D10G to IKKβ

As described above, D10G inhibits the catalytic activities of wild-type IKKβ proteins or IKKβ (SS/EE) immunoprecipitates but not those of IKKβ (C/A) immunoprecipitates, and it suppresses cellular NF-κB activation elicited by a IKKβ (SS/EE) vector but not the IKKβ (C/A) vector. Based on our experimental evidence, we proposed model in which D10G is covalently bound to the crystal structure of human IKKβ (Xu *et al.*, 2011). As shown in Figure 4, D10G was well fitted into the activation loop of IKKβ, displaying a Michael adduct with Cys^{179}, and close contacts with Asn^{54}, Arg^{57}, Leu^{167}, Tyr^{169} and Val^{183} under the most energetically favourable simulation. The methoxy group at the phenyl moiety and the carbonyl group at the C-5 position of D10G achieved hydrogen bonds with side chains of Arg^{57} and Tyr^{169} in the activation loop of IKKβ, respectively.

D10G prevents LPS-induced NF-κB activation

It is important to prove a cross-relationship between IKKβ inhibition and the resultant cellular response. We next assessed LPS-induced signalling events downstream of IκBα phosphorylation that are required for NF-κB activation. Upon exposure to LPS alone, RAW 264.7 cells dramatically degraded IκBα proteins in the cytoplasm within 30–40 min (Figure 5A). Treatment with D10G prevented IκBα degradation in LPS-activated macrophages (Figure 5A); this occurred after IKKβ-catalysed IκBα phosphorylation. Confocal fluorescence

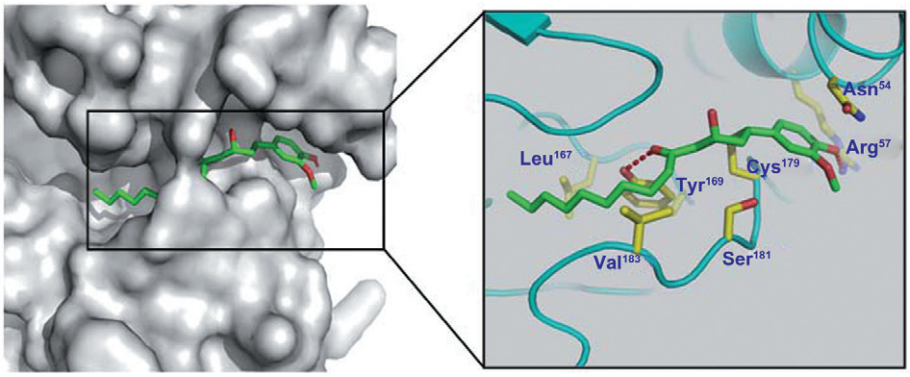

Figure 4

Molecular docking of D10G to IKKβ. A docking arrangement of D10G to the crystal structure of human IKKβ is represented as D10G by green colour and its interacting residues in the activation loop of IKKβ by yellow colour with a covalent linkage to the Cys^{179} of IKKβ. Hydrogen bonding between the Arg^{57} of IKKβ and the methoxy group at phenyl moiety of D10G or between the Tyr^{169} of IKKβ and the carbonyl group at C-5 position of D10G is also indicated as a red dotted line.

analysis revealed another sequential effect of D10G; it prevented NF-κB movement from the cytoplasm to the nucleus. NF-κB was localized within the cytoplasm in cells in media alone, LPS induced the nuclear import of NF-κB p65 and treatment with D10G suppressed this translocation of NF-κB (Figure 5B). We further analysed the transcriptional activity of NF-κB, a hallmark of NF-κB activation. RAW 264.7 cells containing the pNF-κB-SEAP-NPT reporter construct were stimulated with LPS for 20 h in the presence of D10G. Although D10G had no effect on the basal levels of SEAP, it dose-dependently inhibited LPS-induced SEAP expression with an IC_{50} value of 8 μM (Figure 5C). As expected, the IKKβ inhibitor PTN also inhibited LPS-induced SEAP expression (Figure 5C). D10G at concentrations that were effective at inhibiting NF-κB activation did not affect the proliferation of RAW 264.7 cells (Figure 5D), excluding a possible non-specific cytotoxic effect of D10G.

D10G suppresses NF-κB-regulated gene expression

Since D10G inhibited LPS-induced NF-κB activation and also IKKβ (SS/EE) vector-elicited NF-κB transcriptional activity in macrophages, we next asked whether it could suppress the expression of NF-κB-target genes. LPS-responsive κB motifs have been identified on the promoter regions of iNOS with two sites at –8287/–8270 and –119/–102 relative to the transcription start, COX-2 with one site at –223/–214, and IL-6 with one site at –72/–63 (Lowenstein *et al.*, 1993; Zhang *et al.*, 1995; Yeo *et al.*, 2003). Protein levels of iNOS or COX-2 were barely detectable in resting RAW 264.7 cells, as determined by Western blot analysis, but markedly increased upon exposure to LPS alone (Figure 6A). Protein levels of IL-6 were 37 ± 11 $pg{\cdot}mL^{-1}$ in the culture media of resting RAW 264.7 cells (detected by ELISA) and increased to 1483 ± 46 $pg{\cdot}mL^{-1}$ upon exposure to LPS alone (Table 1). Treatment with D10G decreased LPS-inducible protein levels of iNOS and COX-2 (Figure 6A) and those of IL-6 (Table 1). Accordingly, treatment with D10G attenuated LPS-induced mRNA levels of iNOS, COX-2 and IL-6 (Figure 6B). To further understand whether these down-regulatory effects of D10G took place at the transcription level, we transfected RAW 264.7 cells with the piNOS-Luc construct of a luciferase reporter containing an iNOS promoter (–1592/+183) (Lowenstein *et al.*, 1993), or a pCOX-2-Luc reporter construct containing a COX-2 promoter (–963/+1) (Yeo *et al.*, 2003). Upon exposure to LPS alone, these transfected cells increased luciferase expression as a reporter of iNOS or COX-2 promoter activity up to 11- to 15-fold over the basal levels (Figure 6C, D). Treatment with D10G dose-dependently inhibited LPS-induced iNOS promoter activity with an IC_{50} value of 12 μM (Figure 6C) and also COX-2 promoter activity with an IC_{50} value of 14 μM (Figure 6D). We then quantified NO and PGE_2 levels in LPS-activated macrophages to delineate the resultant effects of D10G on the gene expression of iNOS and COX-2, respectively. Treatment with D10G dose-dependently inhibited LPS-induced NO production with an IC_{50} value of 13 μM (Table 1). In a parallel experiment, treatment with D10G also inhibited LPS-induced PGE_2 production with an IC_{50} value of 9 μM (Table 1).

D10G inhibits TNFSF11-elicited NF-κB activation and LPS-induced AP-1 activation

IKKα and IKKβ contain very similar kinase domains with essentially identical activation loops (Mercurio *et al.*, 1997). To understand whether D10G can affect the IKKα-dependent NF-κB activating pathway, we determined NF-κB transcriptional activity and inflammatory mediator production in macrophages stimulated with TNFSF11, an efficient IKKα activator (Affara and Coussens, 2007). Treatment with D10G inhibited TNFSF11-increased SEAP expression, a reporter of NF-κB transcriptional activity, in RAW 264.7 cells containing the pNF-κB-SEAP-NPT construct (Figure 7A). Moreover, treatment with D10G consistently inhibited TNFSF11-induced IL-6 or NO levels in these cells (Figure 7B, C).

Bacterial LPS also activates the activating protein 1 (AP-1) in addition to NF-κB through TLR4 in macrophages (Lu *et al.*, 2008). To investigate whether D10G can inhibit this NF-κB-independent pathway, we determined MAPK activation and

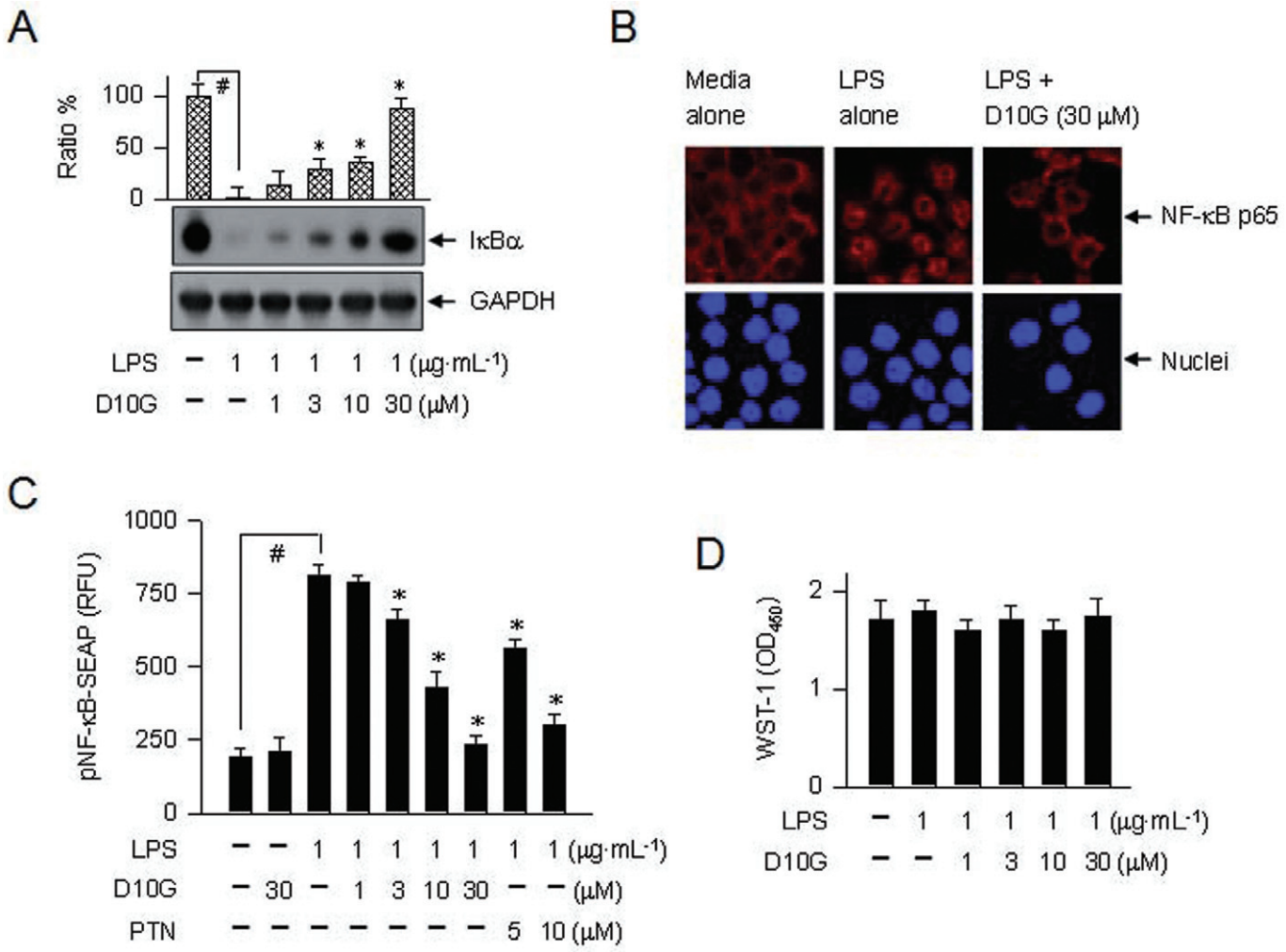

Figure 5

Effect of D10G on the LPS-induced NF-κB activating pathway. (A) RAW 264.7 cells were pretreated with D10G for 2 h and stimulated with LPS for 30–40 min in the presence of D10G. Cell extracts were subjected to Western blot analysis with anti-IκBα or anti-GAPDH antibody. The IκBα levels are presented as the relative ratio %, in which a density of media alone-treated group is expressed as 100%, after normalizing to housekeeping GAPDH levels. (B) RAW 264.7 cells were pretreated with D10G for 2 h and stimulated with LPS (1 μg·mL^{-1}) for 1 h in the presence of D10G. These cells were subjected to confocal fluorescence microscopy, which displays the NF-κB p65-stained with Alexa Fluor 568-labelled antibody as a red colour and the nuclei-stained with DAPI as a blue colour. (C) RAW 264.7 cells containing pNF-κB-SEAP-NPT reporter construct were stimulated with LPS for 20 h in the presence of D10G or parthenolide (PTN). SEAP expression, a reporter of NF-κB transcriptional activity, was measured as RFU. (D) RAW 264.7 cells were incubated with D10G for 24 h in the presence of LPS. Proliferation of the cells was analysed by WST-1 method and is represented as the optical density at wavelength 450 nm (OD_{450}). Data are expressed as mean ± SD of three to five independent experiments. $^{\#}P < 0.05$ versus media alone-added group. $^{*}P < 0.05$ versus LPS alone-stimulated group.

AP-1 transcriptional activity in LPS-stimulated macrophages. Upon exposure to LPS alone, RAW 264.7 cells dramatically increased the phosphorylation of JNK at Thr^{183} and Tyr^{185}, p38 at Thr^{180} and Tyr^{182} and ERK at Thr^{202} and Tyr^{204}; these are activation indexes of each MAPK (Figure S4). Treatment with D10G differentially inhibited LPS-induced MAPK phosphorylation in the cells, in which JNK activation was more sensitive (Figure S4). We next transfected RAW 264.7 cells with pAP-1-Luc construct, a luciferase reporter gene fused to three copies of the AP-1-binding DNA motif. Upon exposure to LPS alone, these transfected cells increased luciferase expression reporting AP-1 transcriptional activity up to 12-fold over the basal levels (Figure S4). Treatment with D10G inhibited LPS-induced AP-1 transcriptional activity in the cells, in which the JNK inhibitor SP600125 was also effective (Figure S4).

Discussion and conclusion

TLRs or antigen receptors activate NF-κB for innate or acquired immunity, in which they transmit signal cascades across the plasma membrane, converging on the IKKβ-catalysed phosphorylation of cytoplasmic IκBα for NF-κB activation even starting from distinct adaptor molecules (Ruland and Mak, 2003; Ospelt and Gay, 2010). Therefore, IKKβ inhibitors are attractive as candidates for the ameliora-

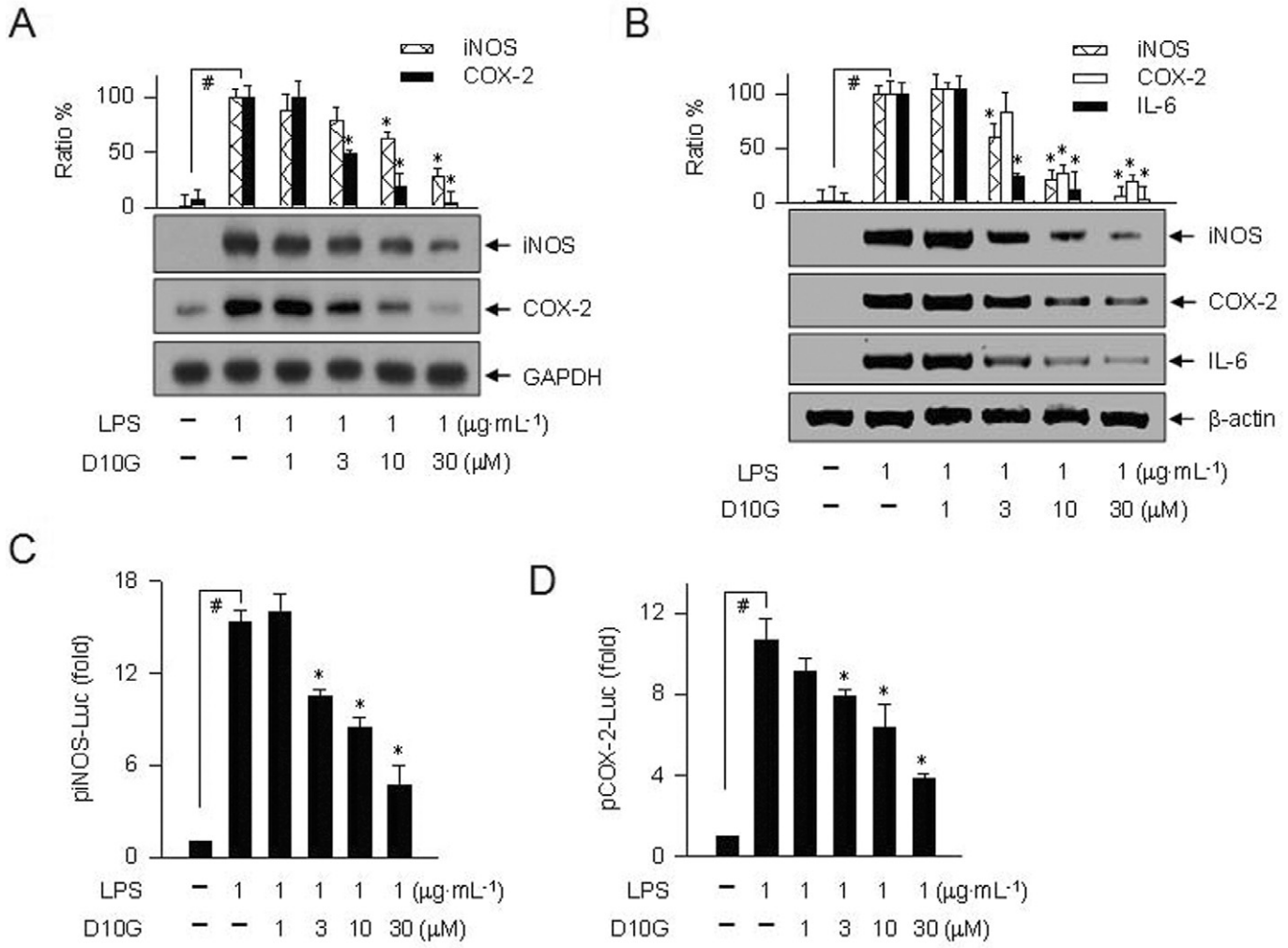

Figure 6

Effect of D10G on LPS-induced expression of inflammatory genes. (A) RAW 264.7 cells were stimulated with LPS for 20 h in the presence of D10G. Cell extracts were subjected to Western blot analysis with anti-iNOS, anti-COX-2 or anti-GAPDH antibody. Protein levels of iNOS or COX-2 are presented as the relative ratio %, in which a density of LPS alone-stimulated group is expressed as 100%, after normalizing to housekeeping GAPDH. (B) RAW 264.7 cells were pretreated with D10G for 2 h and stimulated with LPS for 4–6 h in the presence of D10G. Total RNAs were subjected to RT-PCR analysis. The mRNA levels of iNOS, COX-2 or IL-6 are presented as the relative ratio %, in which a density of LPS alone-stimulated group is expressed as 100%, after normalizing to housekeeping β-actin as an internal control. RAW 264.7 cells were transiently transfected with the reporter construct of piNOS (–1592/+183)-Luc (C) or pCOX-2 (–963/+1)-Luc (D) in combination with *Renilla* control vector. These transfected cells were stimulated with LPS for 20 h in the presence of D10G. Cell extracts were subjected to dual-luciferase assay. Luciferase expression is represented as a relative fold change, in which firefly luciferase activity was normalized to the *Renilla* activity. Data are expressed as mean ± SD of three independent experiments. $^{\#}P < 0.05$ versus media alone-added group. $^{*}P < 0.05$ versus LPS alone-stimulated group.

tion of a broad spectrum of NF-κB-associated inflammatory and autoimmune disorders (Karin *et al.*, 2004). In the present study, we demonstrated that IKKβ is a molecular target of D10G, one of the pungent isolates from ginger, in the inhibition of NF-κB activation and NF-κB-regulated gene expression in macrophages. D10G directly inhibited the Ser/The kinase activity of cell-free IKKβ and the IKKβ-catalysed phosphorylation of cytoplasmic IκBα in macrophages stimulated with agonists of TLR2/6, TLR4 or TLR5. D10G interacted with Cys^{179} in the activation loop of IKKβ, as was evidenced by its selective inhibition of *in vitro* kinase activities of wild-type IKKβ proteins or IKKβ (SS/EE) immunoprecipitates but not those of IKKβ (C/A) immunoprecipitates. Accordingly, D10G inhibited the NF-κB activation elicited by ectopic expression of IKKβ (SS/EE) in macrophages but was ineffective against those elicited by the IKKβ (C/A) vector.

Genetic substitutions of the activation loop Ser^{177} and Ser^{181} residues with Ala decrease IKKβ activity, whereas those of IKKβ (SS/EE) stimulate kinase activity by mimicking Ser phosphorylation (Mercurio *et al.*, 1997; 1999). Interestingly, IKKβ (C/A) decreases its kinase activity, suggesting that Cys^{179} plays an important role in the binding affinity of cofactor ATP with IKKβ and in the Ser phosphorylation of IKKβ to stimulate its kinase activity (Byun *et al.*, 2006). To further understand the molecular mechanism of D10G, we proposed molecular docking of D10G to the crystal structure of human

Table 1

Effect of D10G on LPS-induced production of IL-6, NO and PGE_2

Treatment	IL-6 ($pg \cdot mL^{-1}$)	NO (μM)	PGE_2 ($pg \cdot mL^{-1}$)
Media alone	37 ± 11	1.2 ± 2.6	65 ± 103
LPS alone	1483 ± 46#	34.3 ± 2.3#	3,176 ± 207#
LPS + D10G (1 μM)	1429 ± 48	33.0 ± 3.9	2,523 ± 92*
LPS + D10G (3 μM)	1067 ± 36*	27.3 ± 1.8*	1,827 ± 193*
LPS + D10G (10 μM)	568 ± 19*	22.4 ± 3.0*	1,454 ± 139*
LPS + D10G (30 μM)	258 ± 9*	9.4 ± 1.7*	472 ± 218*

RAW 264.7 cells were stimulated with LPS (1 $\mu g \cdot mL^{-1}$) for 24 h in the presence of D10G. The concentrations of IL-6, NO and PGE_2 were determined in the culture media. Data are expressed as mean ± SD of three to five independent experiments. #$P < 0.05$ versus media alone-added group. *$P < 0.05$ versus LPS alone-stimulated group.

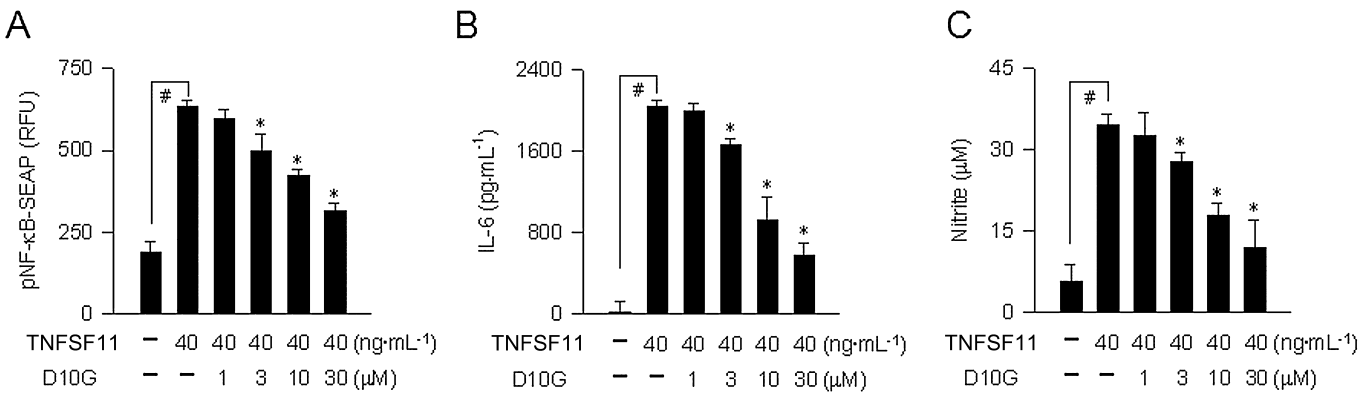

Figure 7

Effect of D10G on TNFSF11-induced NF-κB transcriptional activity and production of IL-6 or NO. (A) RAW 264.7 cells containing pNF-κB-SEAP-NPT reporter construct were stimulated with TNFSF11 for 20 h in the presence of D10G. SEAP expression reporting NF-κB transcriptional activity was measured as RFU. (B, C) RAW 264.7 cells were stimulated with TNFSF11 for 24 h in the presence of D10G. Concentrations of IL-6 or nitrite (a stable metabolite of NO) were determined in the culture media. Data are expressed as mean ± SD of three to five independent experiments. #$P < 0.05$ versus media alone-added group. *$P < 0.05$ versus TNFSF11 alone-stimulated group.

IKKβ. The activation loop of IKKβ was somewhat flexible by itself but subtly rearranged to an extended structure upon irreversible binding of D10G with the Cys^{179} under the most energetically favourable simulation. This conformational change might contribute to the inhibitory mechanism of D10G on IKKβ activity.

Small-molecule inhibitors of IKKβ activity for which a mechanism of action is known can be divided into three general groups: (i) thiol-reactive inhibitors that interact with Cys^{179} in the activation loop of IKKβ, (ii) ATP analogues that target the cofactor-binding site of IKKβ with some specificity and (iii) allosteric inhibitors of IKKβ. In the present study, D10G was a thiol-reactive inhibitor of IKKβ and its effect was abolished by substitution of Cys^{179} with Ala in the activation loop of IKKβ. By this mechanism, D10G was able to inhibit the IKKβ-catalysed phosphorylation of cytoplasmic IκBα in macrophages and to suppress the expression of NF-κB-target inflammatory genes such as iNOS, COX-2 and IL-6 in LPS-activated cells. Arsenic trioxide is an effective drug for the treatment of promyelocytic leukaemia, and its biological effects are confined to structural and functional alterations of critical cellular proteins, including IKKβ due to its reactivity with sulfahydryl groups (Kapahi *et al.*, 2000). Other thiol-reactive inhibitors of IKKβ activity include herbimycin A, cyclopentenone PGs, artemisolide, celastrol, piceatannol and the synthetic triterpenoid 1-[2-cyano-3,12-dioxooleana-1,9(11)-dien-28-oyl]imidazole (Hehner *et al.*, 1999; Kim *et al.*, 2007; Gupta *et al.*, 2010; Son *et al.*, 2010). However, some non-steroidal anti-inflammatory drugs, such as aspirin and sulindac, inhibit IKKβ activity by another mechanism (decreased ATP-binding affinity with IKKβ), which is independent of their well-known effects on COX activity (Yin *et al.*, 1998; Yamamoto *et al.*, 1999). Many pharmaceutical companies have undertaken drug discovery efforts targeting IKKβ. For example, β-carboline PS-1145, quinazoline SPC 839 and aminothiophenecarboxamide SC-514 inhibit IKKβ activity by acting on the ATP-binding site and successfully display pharmacological effectiveness in preclinical arthritis models (Castro *et al.*, 2003; Karin *et al.*, 2004; Schopf *et al.*, 2006). Imidazoquinoxaline BMS-345541 is an allosteric inhibitor of

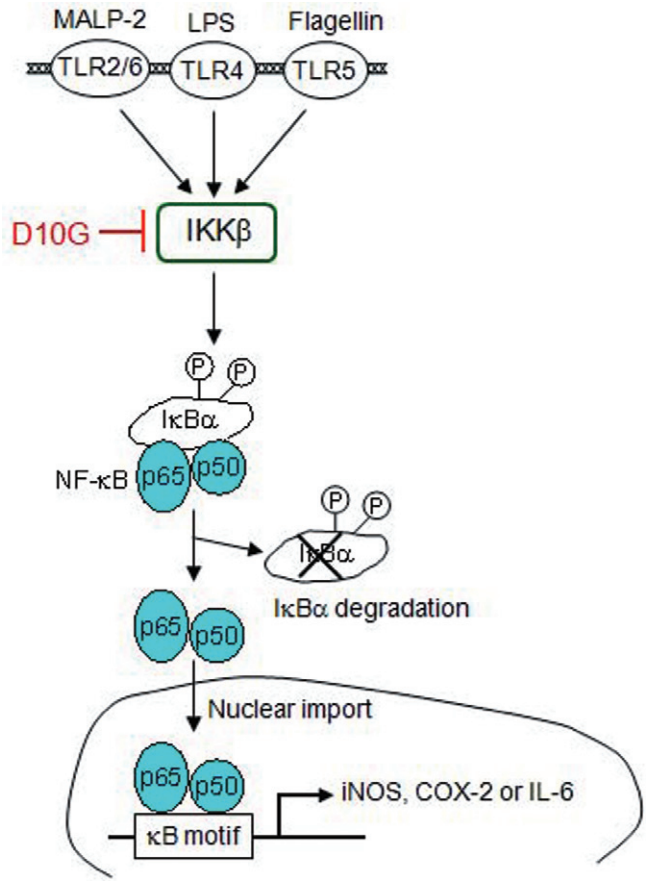

Figure 8

Proposed mechanism for D10G-mediated suppression of NF-κB-regulated gene expression. D10G directly inhibits IKKβ activity, catalysing IκBα phosphorylation in the cytoplasm of macrophages activated by TLR2/6, TLR4 or TLR5 agonist. This mechanism of action disrupts downstream signalling events such as IκBα degradation and the nuclear import of NF-κB in the canonical pathway of NF-κB activation and sequentially suppresses NF-κB-regulated expression of iNOS, COX-2 and IL-6.

IKKβ and prevents collagen-induced arthritis (Burke *et al.*, 2003). In the present study, D10G also inhibited TNFSF11-induced NF-κB activation and LPS-induced AP-1 activation in macrophages. These results suggest that D10G is a muti-kinase inhibitor or targets another signalling molecule in addition to IKKβ for the suppression of TLR-mediated innate immunity.

Taken together, D10G from ginger inhibited the catalytic activity of IKKβ by interacting directly with Cys^{179} in the activation loop of IKKβ. This mechanism of action contributed its ability to inhibit IKKβ-catalysed IκBα phosphorylation, a converging step in the NF-κB activating pathways in macrophages mediated by TLR2/6, TLR4 or TLR5, and sequentially to suppress NF-κB-regulated expression of inflammatory genes such as iNOS, COX-2 or IL-6 in the cells (Figure 8). The current study reveals a new molecular target of D10G that can be evaluated for its therapeutic potential in NF-κB-associated inflammatory and autoimmune disorders. A more complete understanding of the efficacy of IKKβ inhibition in human disease, in addition to its safety evaluation, would be a requisite for small-molecule drug candidates to progress into clinical trials.

Acknowledgements

This work was supported by Core Project (2011–0016211), Priority Research Center Program (2011–0031403) and Medical Research Center Program (2010–0029480) from the National Research Foundation of Korea. We appreciate Dr YS Kim (Seoul National University, Seoul, Korea) for kind supply of pNF-κB-SEAP-NPT construct. Dr JH Lee (Kangwon National University, Chuncheon, Korea) for the expression vectors of IKKβ (SS/EE) and IKKβ (C/A). Dr CJ Lowenstein (Johns Hopkins University School of Medicine, Baltimore, MD) for piNOS-Luc construct and Dr A-K Yi (University of Tennessee Health Science Center, Memphis, TN) for pCOX-2-Luc construct.

Conflicts of interest

The authors state no conflict of interest.

References

Affara NI, Coussens LM (2007). IKKα at the crossroads of inflammation and metastasis. Cell 129: 25–26.

Ali BH, Blunden G, Tanira MO, Nemmar A (2008). Some phytochemical, pharmacological and toxicological properties of ginger (*Zingiber officinale* Roscoe): a review of recent research. Food Chem Toxicol 46: 409–420.

Baeuerle PA, Baltimore D (1988). IκB: a specific inhibitor of the NF-κB transcription factor. Science 242: 540–546.

Bliddal H, Rosetzsky A, Schlichting P, Weidner MS, Andersen LA, Ibfelt HH *et al.* (2000). A randomized, placebo-controlled, cross-over study of ginger extracts and ibuprofen in osteoarthritis. Osteoarthritis Cartilage 8: 9–12.

Burke JR, Pattoli MA, Gregor KR, Brassil PJ, MacMaster JF, McIntyre KW *et al.* (2003). BMS-345541 is a highly selective inhibitor of IκB kinase that binds at an allosteric site of the enzyme and blocks NF-κB-dependent transcription in mice. J Biol Chem 278: 1450–1456.

Byun MS, Choi J, Jue DM (2006). Cysteine-179 of IκB kinase β plays a critical role in enzyme activation by promoting phosphorylation of activation loop serines. Exp Mol Med 38: 546–552.

Castro AC, Dang LC, Soucy F, Grenier L, Mazdiyasni H, Hottelet M *et al.* (2003). Novel IKK inhibitors: β-carbolines. Bioorg Med Chem Lett 13: 2419–2422.

Chung EY, Roh E, Kwak JA, Lee HS, Lee SH, Lee CK *et al.* (2010). α-Viniferin suppresses the signal transducer and activation of transcription-1 (STAT-1)-inducible inflammatory genes in interferon-γ-stimulated macrophages. J Pharmacol Sci 112: 405–414.

DiDonato J, Mercurio F, Rosette C, Wu-Li J, Suyang H, Ghosh S *et al.* (1996). Mapping of the inducible IκB phosphorylation sites that signal its ubiquitination and degradation. Mol Cell Biol 16: 1295–1304.

Fouda AM, Berika MY (2009). Evaluation of the effect of hydroalcoholic extract of *Zingiber officinale* rhizomes in rat collagen-induced arthritis. Basic Clin Pharmacol Toxicol 104: 262–271.

Gupta SC, Sundaram C, Reuter S, Aggarwal BB (2010). Inhibiting NF-κB activation by small molecules as a therapeutic strategy. Biochim Biophys Acta 1799: 775–787.

Hehner SP, Hofmann TG, Droge W, Schmitz ML (1999). The antiinflammatory sesquiterpene lactone parthenolide inhibits NF-κB by targeting the IκB kinase complex. J Immunol 163: 5617–5623.

Kapahi P, Takahashi T, Natoli G, Adams SR, Chen Y, Tsien RY *et al.* (2000). Inhibition of NF-κB activation by arsenite through reaction with a critical cysteine in the activation loop of IκB kinase. J Biol Chem 275: 36062–36066.

Karin M, Ben-Neriah Y (2000). Phosphorylation meets ubiquitination: the control of NF-κB activity. Annu Rev Immunol 18: 621–663.

Karin M, Yamamoto Y, Wang QM (2004). The IKK NF-κB system: a treasure trove for drug development. Nat Rev Drug Discov 3: 17–26.

Kilkenny C, Browne W, Cuthill IC, Emerson M, Altman DG (2010) NC3Rs Reporting Guidelines Working Group. Br J Pharmacol 160: 1577-1579.

Kim BH, Lee JY, Seo JH, Lee HY, Ryu SY, Ahn BW *et al.* (2007). Artemisolide is a typical inhibitor of IκB kinase β targeting cysteine-179 residue and down-regulates NF-κB-dependent TNF-α expression in LPS-activated macrophages. Biochem Biophys Res Commun 361: 593–598.

Kim BH, Roh E, Lee HY, Lee IJ, Ahn B, Jung SH *et al.* (2008). Benzoxathiole derivative blocks lipopolysaccharide-induced nuclear factor-κB activation and nuclear factor-κB-regulated gene transcription through inactivating inhibitory κB kinase β. Mol Pharmacol 73: 1309–1318.

Kim SO, Kundu JK, Shin YK, Park JH, Cho MH, Kim TY *et al.* (2005). [6]-Gingerol inhibits COX-2 expression by blocking the activation of p38 MAP kinase and NF-κB in phorbol ester-stimulated mouse skin. Oncogene 24: 2558–2567.

Kiuchi F, Iwakami S, Shibuya M, Hanaoka F, Sankawa U (1992). Inhibition of prostaglandin and leukotriene biosynthesis by gingerols and diarylheptanoids. Chem Pharm Bull (Tokyo) 40: 387–391.

Koh EM, Kim HJ, Kim S, Choi WH, Choi YH, Ryu SY *et al.* (2009). Modulation of macrophage functions by compounds isolated from *Zingiber officinale*. Planta Med 75: 148–151.

Lee TY, Lee KC, Chen SY, Chang HH (2009). 6-Gingerol inhibits ROS and iNOS through the suppression of PKC-α and NF-κB pathways in lipopolysaccharide-stimulated mouse macrophages. Biochem Biophys Res Commun 382: 134–139.

Levy AS, Simon O, Shelly J, Gardener M (2006). 6-Shogaol reduced chronic inflammatory response in the knees of rats treated with complete Freund's adjuvant. BMC Pharmacol 6: 12.

Lowenstein CJ, Alley EW, Raval P, Snowman AM, Snyder SH, Russell SW *et al.* (1993). Macrophage nitric oxide synthase gene: two upstream regions mediate induction by interferon γ and lipopolysaccharide. Proc Natl Acad Sci USA 90: 9730–9734.

Lu YC, Yeh WC, Ohashi PS (2008). LPS/TLR4 signal transduction pathway. Cytokine 42: 145–151.

McGrath J, Drummond G, Kilkenny C, Wainwright C(2010). Guidelines for reporting experiments involving animals: the ARRIVE guidelines. Br J Pharmacol 160: 1573–1576.

Mercurio F, Zhu H, Murray BW, Shevchenko A, Bennett BL, Li J *et al.* (1997). IKK-1 and IKK-2: cytokine-activated IκB kinases essential for NF-κB activation. Science 278: 860–866.

Mercurio F, Murray BW, Shevchenko A, Bennett BL, Young DB, Li JW *et al.* (1999). IκB kinase (IKK)-associated protein 1, a common component of the heterogeneous IKK complex. Mol Cell Biol 19: 1526–1538.

Moon KY, Hahn BS, Lee J, Kim YS (2001). A cell-based assay system for monitoring NF-κB activity in human HaCat transfectant cells. Anal Biochem 292: 17–21.

Ohto U, Fukase K, Miyake K, Satow Y (2007). Crystal structures of human MD-2 and its complex with antiendotoxic lipid IVa. Science 316: 1632–1634.

Ospelt C, Gay S (2010). TLRs and chronic inflammation. Int J Biochem Cell Biol 42: 495–505.

Pan MH, Hsieh MC, Hsu PC, Ho SY, Lai CS, Wu H *et al.* (2008). 6-Shogaol suppressed lipopolysaccharide-induced up-expression of iNOS and COX-2 in murine macrophages. Mol Nutr Food Res 52: 1467–1477.

Poltorak A, He X, Smirnova I, Liu MY, Van Huffel C, Du X *et al.* (1998). Defective LPS signaling in C3H/HeJ and C57BL/10ScCr mice: mutations in Tlr4 gene. Science 282: 2085–2088.

Ruland J, Mak TW (2003). Transducing signals from antigen receptors to nuclear factor κB. Immunol Rev 193: 93–100.

Schmid JA, Birbach A (2008). IκB kinase β (IKKβ/IKK2/IKBKB): a key molecule in signaling to the transcription factor NF-κB. Cytokine Growth Factor Rev 19: 157–165.

Schopf L, Savinainen A, Anderson K, Kujawa J, DuPont M, Silva M *et al.* (2006). IKKβ inhibition protects against bone and cartilage destruction in a rat model of rheumatoid arthritis. Arthritis Rheum 54: 3163–3173.

Shen H, Tesar BM, Walker WE, Goldstein DR (2008). Dual signaling of MyD88 and TRIF is critical for maximal TLR4-induced dendritic cell maturation. J Immunol 181: 1849–1858.

Son PS, Park SA, Na HK, Jue DM, Kim S, Surh YJ (2010). Piceatannol, a catechol-type polyphenol, inhibits phorbol ester-induced NF-κB activation and cyclooxygenase-2 expression in human breast epithelial cells: cysteine 179 of IKKβ as a potential target. Carcinogenesis 31: 1442–1449.

Tian B, Brasier AR (2003). Identification of a nuclear factor κB-dependent gene network. Recent Prog Horm Res 58: 95–130.

Tripathi S, Bruch D, Kittur DS (2008). Ginger extract inhibits LPS induced macrophage activation and function. BMC Complement Altern Med 8: 1–7.

Xu G, Lo YC, Li Q, Napolitano G, Wu X, Jiang X *et al.* (2011). Crystal structure of inhibitor of κB kinase β. Nature 472: 325–330.

Yamamoto Y, Yin MJ, Lin KM, Gaynor RB (1999). Sulindac inhibits activation of the NF-κB pathway. J Biol Chem 274: 27307–27314.

Yeo SJ, Yoon JG, Yi AK (2003). Myeloid differentiation factor 88-dependent post-transcriptional regulation of cyclooxygenase-2 expression by CpG DNA: tumor necrosis factor-α receptor-associated factor 6, a diverging point in the Toll-like receptor 9-signaling. J Biol Chem 278: 40590–40600.

Yin MJ, Yamamoto Y, Gaynor RB (1998). The anti-inflammatory agents aspirin and salicylate inhibit the activity of IκB kinase-β. Nature 396: 77–80.

Zhang Y, Broser M, Rom W (1995). Activation of the interleukin 6 gene by *Mycobacterium tuberculosis* or lipopolysaccharide is mediated by nuclear factors NF/IL6 and NF-κB. Proc Natl Acad Sci USA 91: 2225–2229.

Supporting information

Additional Supporting Information may be found in the online version of this article:

Figure S1 Inhibitory effects of pungent isolates from ginger on LPS-induced NF-κB transcriptional activity. RAW 264.7 cells containing p-NF-κB-SEAP-NPT reporter construct were stimulated with LPS (1 μg·mL^{-1}) for 20 h in the presence of each compound at concentrations of 10 and 30 μM. A reporter of NF-κB transcriptional activity was measured by SEAP activity and is represented as inhibition %, compared with the LPS alone-stimulated group. Data are expressed as mean ± SD of three independent experiments. **P* < 0.05 versus LPS alone-stimulated group.

Figure S2 HPLC-DAD chromatogram of 1-dehydro-[10]-gingerdione (D10G). HPLC analysis was performed on a Water system (2996 photodiode array detector with two 515 pumps) and a YMC J'sphere ODS-H80 column (4 μm, 150 × 20 mm), using the mixed solvent system CH_3CN-H_2O (50:50 to 100:0) at a flow rate of 1.0 mL·min^{-1}.

Figure S3 Electrophilic moieties in the chemical structures of parthenolide and D10G.

Figure S4 Effect of D10G on LPS-induced MAPK activation and AP-1 transcriptional activity. (A) RAW 264.7 cells were pretreated with D10G for 2 h and stimulated with LPS for 30 min in the presence of D10G. Cell extracts were subjected to Western blot analysis with pairs of antibodies against p-JNK and JNK, p-p38 and p38 or p-ERK and ERK. (B) RAW 264.7 cells were transfected with pAP-1-Luc, an AP-1-dependent luciferase reporter construct, in combination with *Renilla* control vector. These transfected cells were stimulated with LPS for 20 h in the presence of D10G or SP600125. Cell extracts were subjected to dual-luciferase assay. Luciferase expression is represented as a relative fold, in which firefly luciferase activity was normalized to *Renilla* activity. Data are expressed as mean ± SD of three independent experiments. $^{\#}P$ < 0.05 versus media alone-added group. **P* < 0.05 versus LPS alone-stimulated group.

Please note: Wiley-Blackwell are not responsible for the content or functionality of any supporting materials supplied by the authors. Any queries (other than missing material) should be directed to the corresponding author for the article.